THE JOURNAL OF BIOLOGICAL CHEMISTRY VOL. 286, NO. 7, pp. 5876–5883, February 18, 2011

ATP Modulates Interaction of Syntaxin-1A with Sulfonylurea Receptor 1 to Regulate Pancreatic β-Cell K_{ATP} Channels*[S]

Received for publication, November 26, 2009, and in revised form, November 23, 2010 Published, JBC Papers in Press, December 20, 2010, DOI 10.1074/jbc.M109.089607

Youhou Kang[‡1], Yi Zhang[‡1], Tao Liang[‡1], Yuk-Man Leung[‡], Betty Ng[‡], Huanli Xie[‡], Nathan Chang[‡], Joseph Chan[‡], Show-Ling Shyng[§], Robert G. Tsushima[¶], and Herbert Y. Gaisano[‡2]

From the [‡]Department of Medicine, University of Toronto and University Health Network, Toronto, Ontario M5S 1A8, Canada, the [§]Center for Research on Occupational and Environmental Toxicology Oregon Health and Science University, Portland, Oregon 97239, and the [¶]Department of Biology, York University, Toronto, Ontario M3J 1P3, Canada

ATP-sensitive potassium (K_{ATP}) channels are regulated by a variety of cytosolic factors (adenine nucleotides, Mg^{2+}, phospholipids, and pH). We previously reported that K_{ATP} channels are also regulated by endogenous membrane-bound SNARE protein syntaxin-1A (Syn-1A), which binds both nucleotide-binding folds of sulfonylurea receptor (SUR)1 and 2A, causing inhibition of K_{ATP} channel activity in pancreatic islet β-cells and cardiac myocytes, respectively. In this study, we show that ATP dose-dependently inhibits Syn-1A binding to SUR1 at physiological concentrations, with the addition of Mg^{2+} causing a decrease in the ATP-induced inhibitory effect. This ATP disruption of Syn-1A binding to SUR1 was confirmed by FRET analysis in living HEK293 cells. Electrophysiological studies in pancreatic β-cells demonstrated that reduced ATP concentrations increased K_{ATP} channel sensitivity to Syn-1A inhibition. Depletion of endogenous Syn-1A in insulinoma cells by botulinum neurotoxin C1 proteolysis followed by rescue with exogenous Syn-1A showed that Syn-1A modulates K_{ATP} channel sensitivity to ATP. Thus, our data indicate that although both ATP and Syn-1A independently inhibit β-cell K_{ATP} channel gating, they could also influence the sensitivity of K_{ATP} channels to each other. These findings provide new insight into an alternate mechanism by which ATP regulates pancreatic β-cell K_{ATP} channel activity, not only by its direct actions on Kir6.2 pore subunit, but also via ATP modulation of Syn-1A binding to SUR1.

The ATP-sensitive potassium (K_{ATP})[3] channel couples intracellular metabolic changes to plasma membrane electrical activity in many cell types (1–3). In pancreatic β-cells, increase in ATP/ADP ratio from glucose metabolism closes plasma membrane K_{ATP} channels, causing membrane depolarization that leads to opening of L-type voltage-dependent calcium channels. Ensuing calcium influx triggers exocytosis of docked and primed insulin granules in part by acting on the exocytic SNARE (soluble NSF attachment protein receptor) complex (4). The pancreatic β-cell K_{ATP} channel is a hetero-octamer of pore-forming Kir 6.2 and regulatory sulfonylurea receptor 1 (SUR1) subunits, with a 4:4 stoichiometry (5–7). SURs are members of the ATP-binding cassette protein superfamily (8), including cystic fibrosis transmembrane conductance regulator and P-glycoprotein/MDR1 (multidrug resistance 1). These ATP-binding cassette proteins uniformly contain two nucleotide-binding folds (NBF1 and NBF2), with each NBF containing Walker A and B motifs, which are sites of the action by adenine nucleotides. Regulation of K_{ATP} channels by adenine nucleotides is complex, with ATP and ADP having both stimulatory and inhibitory effects (9–11). Structure-function studies have demonstrated that ATP inhibits channel activity by interactions with Kir6.2 (12), whereas ADP acts on the SUR subunit to stimulate channel activity in an Mg^{2+}-dependent manner (13).

The importance of SUR1 as a regulator of K_{ATP} channel activity is demonstrated by the fact that loss-of-function mutations decrease K_{ATP} channel activity, leading to continuous insulin secretion, thus causing hyperinsulinism of infancy (14). Conversely, gain-of-function mutations enhance channel activity, leading to reduction of insulin secretion, thereby causing neonatal diabetes (15). SUR1 regulates K_{ATP} channel activity through several mechanisms: modulating channel pore opening kinetics by enhancing channel sensitivity to ATP and open probability (16), enabling functional expression of the channel at the cell surface (17) and conferring channel sensitivity to MgATP, MgADP and therapeutic drugs (sulfonylureas) (12).

In addition to adenine nucleotides, K_{ATP} channels can also be regulated by a variety of cytosolic factors, including phospholipids (18), long-chain acyl-coenyzme A esters (19), and pH (20). These cytosolic factors undergo dynamic changes in pancreatic β-cells in health and diabetes. Remarkably, we have reported that pancreatic β-cell K_{ATP} channels can also be regulated by endogenous plasma membrane-bound syntaxin-1A (Syn-1A), a SNARE protein originally described to mediate exocytic membrane fusion. In contrast to the cytosolic factors that act on the Kir6.2 subunit (18–20), Syn-1A binds the SUR subunits at both NBFs to regulate K_{ATP} channel gating (21, 22).

* This work was supported by a grant from the Canadian Institutes for Health Research (MOP 69083), the Heart and Stroke Foundation of Ontario (T-6064) (to H. Y. G.), and the National Institutes of Health (R01DK066485 to S.-L. S.).

[S] The on-line version of this article (available at http://www.jbc.org) contains supplemental Fig. 1.

[1] These authors contributed equally to this article.

[2] To whom correspondence should be addressed: University of Toronto, 1 King's College Circle, Rm. 7368, Toronto, ON M5S 1A8, Canada. Tel.: 416-978-1526; Fax: 416-978-8765; E-mail: herbert.gaisano@utoronto.ca.

[3] The abbreviations used are: K_{ATP} channel, ATP-sensitive potassium channel; SUR1, sulfonylurea receptor 1; NBF, nucleotide binding fold; Syn-1A, syntaxin-1A; BoNT/C1, botulinum neurotoxin C1; EGFP, enhanced GFP.

In the present study, we examined the interplay between cytosolic ATP and membrane-bound Syn-1A on regulating K_{ATP} channel gating. We show that ATP and Syn-1A influence β-cell K_{ATP} channel sensitivity to each other, with physiological ATP concentrations disrupting the Syn-1A binding to SUR1.

MATERIALS AND METHODS

Constructs and Recombinant GST-fusion Proteins—pGEX-4T-1-Syn-1A was a gift from W. Trimble (The Hospital for Sick Children, Toronto, ON, Canada), pCMV-Syn-1A from R. Scheller (Genentech, Inc., San Francisco, CA), PECE-SUR1-EGFP from C. G. Nichols (Washington University School of Medicine, St. Louis, MO), pECE-Kir6.2 from S. Seino (Chiba University, Chiba, Japan), pcDNA-mCherry from D. Lodwick (University of Leicester, Leicester, Canada), pCMV-BoNT/C1 (botulinum neurotoxin C1) from H. Niemann (Medizinische Hochschule, Hannover, Germany), and pEGFP-N3 was purchased from Clontech (Palo Alto, CA). The full-length Syn-1A cDNA was amplified by PCR, and then the amplified fragment was inserted into pcDNA3-mCherry to create the plasmid pcDNA3-Syn-1A-mCherry. GST-fusion protein expression and purification were performed following the manufacturer's instructions (GE Healthcare).

Cell Culture and Transfection—BA8 cells, stably expressing Kir6.2/SUR1 (23), were cultured in DMEM (Invitrogen) containing 4.5 g/liter glucose and supplemented with 10% FBS (HyClone, Omaha, NE), 0.6 mg/ml G418 and 44 μg/ml hygromycin (both from Sigma). HEK293 cells were cultured in the same DMEM but without G418 and hygromycin and INS-1E cells in RPMI 1640 medium (Invitrogen) supplemented with 10% FBS. HEK293 and INS-1E cells were transiently transfected with Syn-1A or BoNT/C1 or co-transfected with both plasmids using Lipofectamine 2000 (Invitrogen) according to the manufacturer's instructions. 18–24 h after transfection, the cells were harvested for Western blotting, or cells were trypsinized, plated on glass coverslips, and cultured overnight before performing electrophysiological experiments. For FRET imaging, HEK293 cells were co-transfected with Syn-1A-mCherry, SUR1-EGFP, and Kir6.2 or with EGFP and mCherry (control). The cells were used for FRET imaging 2 days after transfection.

In Vitro Binding Assay and Western Blotting—*In vitro* binding assays were performed according to the methods we described previously (22). Briefly, GST (as a negative control) and GST-Syn-1A (350 pmol protein each) were bound to glutathione-agarose beads and incubated with 0.5 ml SUR1 overexpressing HEK293 cell lysate extract (400 μg protein in lysis buffer containing 20 mM HEPES (pH 7.4), 100 mM KCl, 1.5% Triton X-100, 1 μg/ml pepstatin A, 1 μg/ml leupeptin, and 10 μg/ml aprotinin) in the presence or absence of different concentrations of ATP (Sigma) along with or without 2 mM $MgCl_2$ at 4 °C for 2 h with constant agitation, followed by washing the beads three times with washing buffer containing 20 mM HEPES (pH 7.4), 150 mM KOAC, 1 mM EDTA, 5% glycerol, and 0.1% Triton X-100. The samples were then separated on 10% SDS-PAGE, transferred to nitrocellulose membrane, and identified with specific primary antibodies against SUR1 (1:1000; a gift from J. Ferrer, Barcelona, Spain). The blots were quantified by densitometry scanning followed by analysis with Scion Image (beta release version 4.0.2; Scion Corp.). Data analysis and curve fitting were performed using Origin (version 6.0; Microcal Software Inc.).

FRET Imaging—Transfected cells were imaged in intracellular buffer containing 20 mM HEPES, 5 mM NaCl, 140 mM K-gluconate, and 2 mM $MgCl_2$ and pre-equilibrated with O_2:CO_2 = 95:5, pH 7.4 at 37 °C using a Nikon TE-2001U inverted microscope fitted with an argon laser unit (480 ± 10 nm, Spectra-Physics), an He-Ne laser unit (545 ± 10 nm, Melles Griot), and a Quantum 512SC charge-coupled device camera (Photometrics). For FRET measurements, a Plan Apo 60× oil immersion objective (1.65 numerical aperture), a Dual-View imaging system (Optical Insights) containing a dichroic splitter (565dcxr) and two emission filters (HQ530/30 for EGFP and HQ630/50 for mCherry) were combined together to allow simultaneous two-channel monitoring of emission fluorescence. The cells were permeabilized by incubation in intracellular buffer containing 10 μM digitonin for 4 min at 37 °C and then were applied for FRET imaging in the absence or presence of 0.5 or 2 mM ATP. For FRET analysis, EGFP fused with SUR1 was used as FRET donor and mCherry fused with Syn-1A as an acceptor. Four images, including donor excitation/donor emission (*Dd*), donor excitation/acceptor emission, acceptor excitation/acceptor emission (*Aa*), and acceptor excitation/donor emission were acquired in the same condition and a fixed 500-ms exposure time in each FRET experiment. In addition, the donor-only sample and acceptor-only sample were imaged before each experiment for calculation of bleed-through. FRET efficiency was used to indicate the interaction of the two proteins, calculated as follows: $FRET_{corr} = FRET_{raw} - (CoB \times Dd_{FRET}) - (CoA \times Aa_{FRET})$. FRET efficiency % = $(FRET_{corr}/Dd_{FRET}) \times 100\%$. Here, *CoA* is the amount of acceptor bleed-through in the absence of a donor, and *CoB* is the amount of donor bleed-through in the absence of an acceptor.

Electrophysiology—Rat islet β-cells isolated from male Sprague-Dawley as described previously were voltage-clamped in a whole-cell configuration (23). The typical pipette resistance was 3–5 MΩ. The external solution contained the following: 140 mM NaCl, 4 mM KCl, 1 mM $MgCl_2$, 2 mM $CaCl_2$, 2 mM glucose, 10 mM HEPES, pH 7.4 with NaOH. The pipette solution contained the following: 140 mM KCl, 1 mM $MgCl_2$, 1 mM EGTA, 0.3 or 1.0 mM MgATP, and 10 mM HEPES, pH 7.3 with KOH. GST or GST-Syn-1A fusion proteins (all at 1 μM) were added to the pipette solution for dialysis into the cells. Membrane potential was held at −80 mV and a pulse of −140 mV (500 ms) was given every 10 s to monitor K_{ATP} current magnitude. As the pipette contained a low concentration of ATP (when adding 0.3 or 1.0 mM MgATP), which gradually equilibrated with cell cytosol, K_{ATP} currents gradually developed to the maximum amplitude.

INS-1E cells (a gift from C. Wollheim, Geneva, Switzerland) were used for standard inside-out patch-clamp recordings. The cells were transfected with EGFP and BoNT/C1 (to cleave endogenous Syn-1A) or EGFP alone as indicated under "Results." To increase macroscopic K_{ATP} currents, all cells

were subsequently co-infected with three recombinant adenoviruses containing Kir6.2, tetracycline-inhibited transactivator, and tetracycline-inhibited transactivator-regulated gene expressing fSUR1 (FLAG epitope-tagged SUR1) (24). 24 h after infection, the cells were patch clamped in symmetrical K^+ conditions (140 mM KCl, 1 mM EGTA, 1 mM EDTA, and 10 mM HEPES, pH 7.4) with or without MgATP, as indicated. The typical pipette resistance when filled with solution was 1.0–1.5 MΩ. Syn-1A or GST recombinant proteins were added to bath solutions as indicated. Macroscopic currents were recorded with membrane patches held at −50 mV to evoke inward currents. All electrophysiological experiments were performed at room temperature (22–24 °C) using an EPC9 amplifier with Pulse acquisition software (version 8.6; HEKA Electroniks, Mahone Bay, Nova Scotia, Canada).

Data Analysis—Data are presented as means ± S.E. Differences in means were compared using unpaired (electrophysiological studies) or paired (FRET assay) Student's *t* test, with $p < 0.05$ considered as statistically significant.

RESULTS

ATP Dose-dependently Inhibits Syn-1A Binding to SUR1—Our previous studies (22, 23) showed that Syn-1A binds SUR1 at its NBF1 and NBF2 domains and would not bind Kir6.2. In addition, the physical interaction between SNAP-25 and SUR1 was not observed. These results indicate that the interaction of Syn-1A with NBFs of SUR1 does not require a ternary protein. Because ATP (and ADP), in addition to its direct actions on Kir6.2, can also bind NBFs to modulate K_{ATP} channel activity, we speculated that ATP might induce conformational changes in the NBFs, which could influence SUR1 binding to Syn-1A with consequent effects on K_{ATP} channel gating.

First, we used GST-Syn-1A bound to agarose glutathione beads to pull down SUR1 from SUR1/Kir6.2 stably expressing BA8 cell lysate extract in the presence of increasing concentrations of ATP. As shown in Fig. 1*A*, ATP (without Mg^{2+}) dose-dependently inhibited the binding of Syn-1A to SUR1 ($n = 4$). As Mg^{2+} is present physiologically to influence ATP actions, we examined ATP inhibition of Syn-1A binding to SUR1 in the presence of a cellular level of Mg^{2+}. Addition of 2 mM $MgCl_2$ shifted the dose-response curve to higher ATP concentrations (Fig. 1*B*), suggesting a reduction in the ATP-induced inhibitory effect on Syn-1A binding to SUR1. The actions of Mg^{2+} in regulating K_{ATP} channels are complex, and in particular, MgATP would activate K_{ATP} channels, thus counteracting free ATP inhibition of K_{ATP} channels (9, 25). We, therefore, calculated free [Mg^{2+}], free [ATP], and [MgATP] using the Maxchelator program. It appears that it is increasing [MgATP] and not free Mg^{2+} that accounted for, at least in part, the rightward shift in free ATP inhibition of Syn-1A binding to SUR1. For example, at the estimated free ATP concentration of 3 mM, with 2 mM $MgCl_2$, calculated MgATP was 1.94 mM, whereas free [Mg^{2+}] was only 60 μM (Fig. 1*B*), suggesting that free Mg^{2+} in this condition may not be relevant; and this caused a 48% inhibition (Fig. 1*B*), whereas in absence of Mg^{2+} (Fig. 1*A*), the estimated inhibition was stronger at ~74%. At lower [ATP] of 0.5–1 mM,

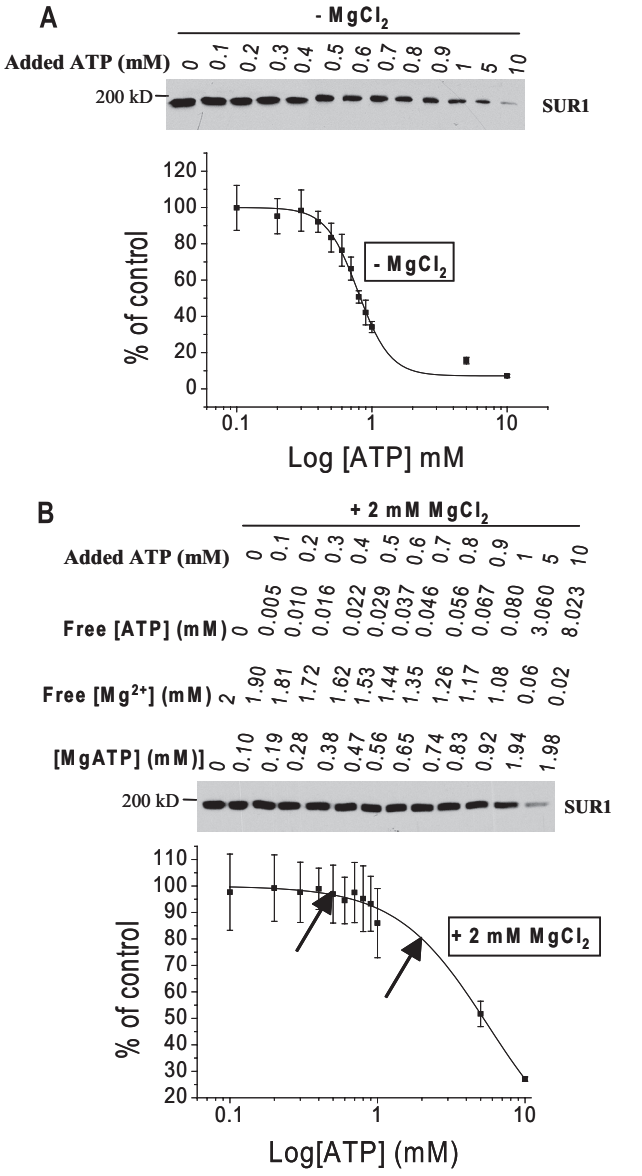

FIGURE 1. **ATP dose-dependently inhibited Syn-1A binding to SUR1.** GST-Syn-1A bound to glutathione-agarose beads was used to pull down SUR1 from SUR1/Kir6.2 expressing HEK293 cell lysate extract in the presence of increasing concentrations of ATP along with (*A*) or without (*B*) 2 mM $MgCl_2$. The *top panels* in *A* and *B* show representative blots, and the *bottom panels* are the summaries of quantitative densitometry scanning of the specific bands. Free [ATP], free [Mg2+], and [MgATP] were calculated and shown on the *top* of the representative blot in *B*. The value from the assay in the absence of ATP and $MgCl_2$ was considered as 100% (control). The results are expressed as mean ± S.E. ($n = 3$). The *arrows* in *B* point to the ATP concentrations (0.5 and 2 mM, respectively) which were used in the FRET study (Fig. 2).

where we observed significant effects on SUR1-Syn-1A binding in the absence of Mg^{2+} (Fig. 1*A*), adding 2 mM $MgCl_2$, greatly reduced these effects, causing a rightward shift of the dose response (Fig. 1*B*), and here, the calculated free [Mg^{2+}] in these conditions, which ranged between 1.1–1.5 mM are quite similar and close to the physiologic values of free [Mg^{2+}] reported in the literature (26). We have indicated two arrows in Fig. 1*B* corresponding to the [ATP] (0.5 and 2 mM, respectively) in the presence of 2 mM $MgCl_2$ used in the FRET studies in Fig. 2. As a negative control, GST did not bind to Syn-1A in all conditions tested (data not shown).

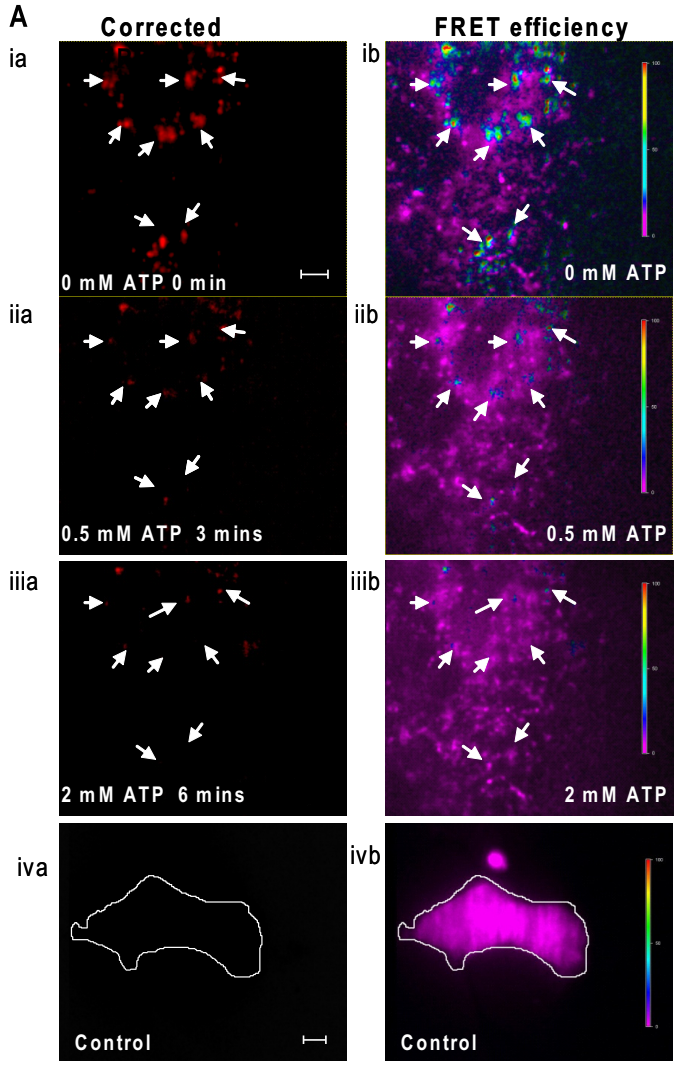

FIGURE 2. **ATP inhibited Syn-1A interaction with SUR1 in living cells.** Shown in *A* (*ia*), *A* (*iia*), and *A* (*iiia*) are representative recordings of the FRET signals on the membrane of a same HEK cell expressing Syn-1A-mCherry, SUR1-EGFP, and Kir6.2 prior to (*A*, *ia*) and after addition of 0.5 (*A*, *iia*) and then 2 mM ATP (*A*, *iiia*), each for 3 min. The excitation wavelength was 488 nm, and fluorescence emission was measured at 605–655 nm. The *arrows* indicate the area where FRET signals decreased significantly after applying ATP. The *bar* indicates 5 μm. *A* (*ib*), *A* (*iib*), and *A* (*iiib*), the FRET efficiency in the same cell corresponding to *A* (*ia*), *A* (*iia*), and *A* (*iiia*), respectively. The *vertical scale bar* indicates the FRET efficiency in pseudocolor. *A* (*iva*) and *A* (*ivb*), FRET signal recording and efficiency in control cells expressing EGFP and mCherry. *B*, summary of FRET efficiency before and after addition of 0.5 or 2 mM ATP. ***, $p < 0.001$ compared with 0 ATP ($n = 12$). *NS*, no significant difference.

ATP Disrupts Syn-1A Binding to SUR1 in Living Cells—Because Syn-1A is known to be a "sticky" protein that could bind nonspecifically to other proteins in protein-binding assays, we proceeded to examine the specific interaction in living cells expressing these interacting proteins in their physiological configuration targeted to their native compartment, the plasma membrane. These proteins were fluorophore-tagged (EGFP or mCherry) and their *bona fide* cellular interactions were examined by FRET analysis in the presence and absence of ATP. HEK293 cells were co-transfected with SUR1 tagged with EGFP as a donor and Syn-1A tagged with mCherry as an acceptor, plus Kir6.2 for complete and functional K_{ATP} channel expression at the plasma membrane. A previous study has shown that spectral properties of EGFP and mCherry are well suited for measuring molecular rearrangements by the FRET technique (27). Due to some overlap in EGFP and mCherry spectra, measured mCherry emission caused by FRET was contaminated by both direct excitation of mCherry and by EGFP cross-talk emission in the mCherry range. To overcome this problem, a sensitive spectral method for FRET efficiency quantification was used as described under "Materials and Methods." To examine the molecular interactions of Syn-1A and SUR1 on the surface of the plasma membrane, we used total internal reflection fluorescence microscopy to optically isolate the plasma membrane, enabling high spatial image resolution of the protein interactions on the entire surfaces of the plasma membrane. Total internal reflection fluorescence microscopy, with an exponentially decaying evanescent wave, illuminates the FRET signal within a thin layer (< 200 nm) at and beneath the plasma membrane, thus significantly reducing out-of-focus background fluorescence.

First, we examined the FRET in HEK293 cells co-transfected with SUR1-EGFP, Syn-1A-mCherry and Kir6.2, and permeabilized with digitonin in the buffer without ATP. We applied a 488-nm laser to excite EGFP and then recorded the mCherry signal (FRET) with a 605–655 nm band-pass filter, which elicited strong FRET signals on the plasma membrane of the cell (Fig. 2, *A*, *ia*), indicating very close proximity between SUR1 and Syn-1A, and thus their presumed interactions. The FRET efficiency, expressed as the mean value of $FRET_{corr}/Dd_{FRET}$, was 44.20 ± 3.91% ($n = 12$) (Fig. 2, *A*, *ib*, and *B*). Note that the discrete punctuate spots indicated by arrows showing the highest FRET signals. When 0.5 mM ATP (in presence of 2 mM $MgCl_2$, giving free [ATP] = 0.04 mM, free [Mg^{2+}] = 1.54 mM, and [MgATP] = 0.46 mM) was applied to these permeabilized HEK cells for 3 min, we observed a dramatic decrease in the FRET signal (purple indicating background FRET) precisely at the same high FRET spots (indicated by *arrows*, compare Fig. 2, *A*, *ia* with 2, *A*, *iia*, and Fig. 2, *A*, *ib*, with 2, *A*, *iib*). Specifically, FRET efficiency decreased by 55.2% from 44.2 ± 3.91% to 19.8 ± 2.32% (Fig. 2*B*). Then, 2 mM ATP (in presence of 2 mM $MgCl_2$, giving free [ATP] = 0.44 mM, free [Mg2+] = 0.44 mM, and [MgATP] = 1.56 mM) was applied to the same cells for another 3 min, and no significant decrease in FRET efficiency was observed (from 19.8 ± 2.32 to 15.3 ± 1.88, $p > 0.05$) (Fig. 2, *A*, *iiia*, 2, *A*, *iiiB*, and Fig. 2*B*). As a negative control, no FRET signal was ob-

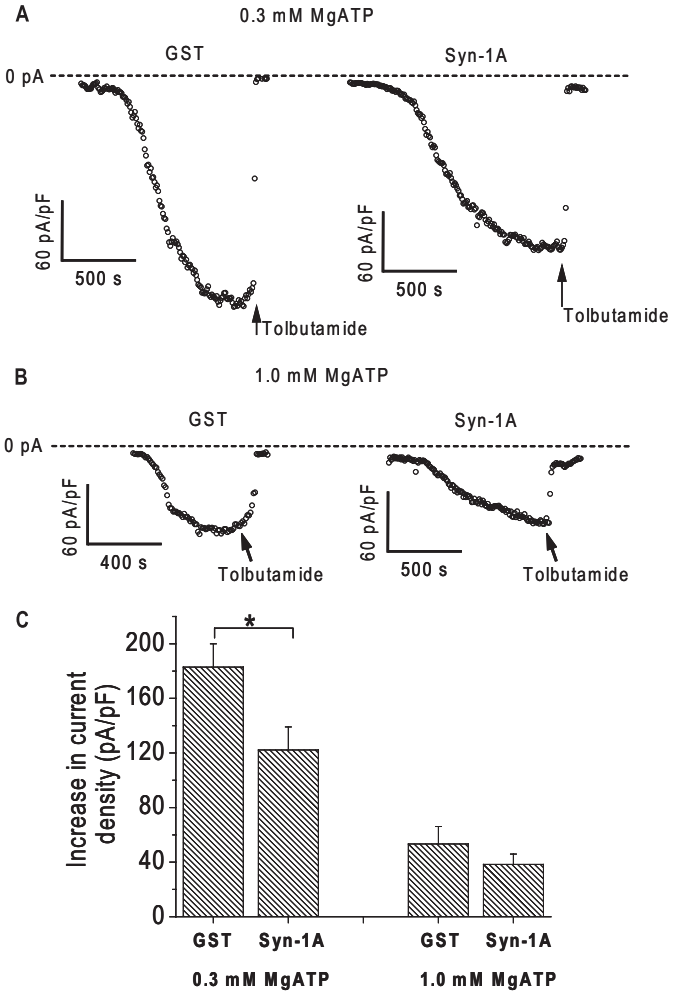

FIGURE 3. **Syn-1A inhibited rat islet β-cell K_{ATP} currents in the presence of 0.3 but not 1 mM intracellular ATP.** Cells were treated with 1 μM Syn-1A or 1 μM GST under whole-cell patch clamp recording mode. *A*, time course of K_{ATP} currents recorded in the presence of 0.3 mM intracellular MgATP. K_{ATP} currents were confirmed by application of 300 μM tolbutamide as indicated by *arrows*. *B*, time course of K_{ATP} currents in the presence of 1.0 mM intracellular MgATP. *C*, summary of the results. The maximum current magnitude was normalized with cell size to yield current density (pA/pF). *, significant difference compared with the control ($p < 0.05$). Results are expressed as mean ± S.E. ($n = 6–11$).

served in HEK293 cells co-transfected with EGFP and mCherry (Fig. 2, *B*, *iva*), showing 0% FRET efficiency (Fig. 2, *A*, *ivb*).

Syn-1A Inhibits Rat Islet β-Cell K_{ATP} Channel Currents at Low but Not High ATP Concentrations—Because our binding studies showed that increasing ATP concentration inhibited Syn-1A binding to SUR1, we examined whether Syn-1A inhibition of pancreatic β-cell K_{ATP} currents could be modified by similar physiological changes in cytosolic ATP concentrations. At low ATP concentration (0.3 mM MgATP in the presence of 1 mM $MgCl_2$ giving free [ATP] = 0.03 mM, free [Mg2+] = 0.94 mM and [MgATP] = 0.27 mM, which did not affect Syn-1A binding to SUR1 in Fig. 1*B*) in the patch pipette, K_{ATP} currents gradually developed in rat β-cells, reaching a maximum current density of 183 ± 17 pA/pF (picoampere/picofarad) (Fig. 3). Dialyzing 1 μM Syn-1A into the cell reduced the currents by 33% (Fig. 3, *A* and *C*), similar to our previous report (23). Addition of a higher concentration of 1 mM MgATP (in presence of 1 mM $MgCl_2$, giving free [ATP] = 0.10 mM, free [Mg^{2+}] = 1.00 mM and [MgATP] = 0.90 mM) in the pipette, maximum current density developed was 53 ± 13 pA/pF. However, dialyzing 1 μM Syn-1A into the cells did not significantly reduce the currents (Fig. 3, *B* and *C*), though the kinetics of current development (Fig. 3*B*) appeared slower than control. Thus, addition of 1 mM MgATP shown to cause only moderate inhibition of Syn-1A binding to SUR1 (Fig. 1*B*) was sufficient to abrogate Syn-1A inhibition of the β-cell K_{ATP} channel. Taken together, these results indicate that reduced cellular ATP concentration enhances β-cell K_{ATP} channel sensitivity to Syn-1A inhibition.

Dynamic Interaction of Endogenous Syn-1A and ATP in Regulation of β-Cell K_{ATP} Channels—We then explored whether endogenous Syn-1A levels could influence β-cell K_{ATP} channel sensitivity to ATP. This is of clinical relevance as islet Syn-1A in diabetics has been shown severely reduced by 79% (28). Here, we depleted endogenous Syn-1A in INS-1E cells by transfection of the cells with BoNT/C1 and EGFP, the latter to identify the BoNT/C1-transfected cells. EGFP alone-transfected cells were used as control. We also performed parallel transfection of HEK293 cells with Syn-1A. 48 h after transfection, Syn-1A was observed to be cleaved completely in INS-1E cells (Fig. 4, *Aii*) and with only a small residual Syn-1A (85% reduction) in Syn-1A-overexpressing HEK293 cells (Fig. 4, *Ai*).

Next, we performed inside-out patch recording on the INS-1E cells to test the effects of different ATP concentrations. Note that K_{ATP} channels from inside-out patches are known to be much more sensitive (*i.e.* 7–26 times) to ATP than those in whole cell configuration in part due to reduced levels of inositol phospholipids (3, 29); hence, we used lower ATP concentrations. As shown in Fig. 4, *B–D*, membrane patches were first exposed to 500 μM MgATP (free [ATP] = 193.9 μM, free [Mg2+] = 175.4 μM, and [MgATP] = 306.6 μM) to close the channel, followed by 0 μM ATP to obtain maximum K_{ATP} currents (I_{max}). Patches were then held at various concentrations of ATP in sequential presence of GST (0.3 μM, indicated as *open bars*) or exogenous Syn-1A (0.3 μM, indicated as *solid bars*). In both BoNT/C1-transfected and control cells, 1 μM MgATP (free [ATP] = 0.99 μM, free [Mg2+] = 0.90 μM, and [MgATP] = 0.01 μM) caused partial K_{ATP} channel inhibition and addition of 20 μM MgATP (free [ATP] = 17.5 μM, free [Mg2+] = 15.8 μM, and [MgATP] = 2.5 μM) induced further inhibition of the K_{ATP} channels. The differences (Δ) in K_{ATP} currents between applications of GST and Syn-1A were determined at 1 μM MgATP (Δ_1) and 20 μM MgATP (Δ_2).

In control cells (Fig. 4, *Bi*), addition of exogenous Syn-1A did not affect K_{ATP} currents compared with GST at either 1 μM MgATP (Δ_1) or 20 μM MgATP (Δ_2). In contrast, in BoNT/C1-transfected cells (Fig. 4, *Ci*), application of 0.3 μM exogenous Syn-1A caused much further K_{ATP} channel inhibition at 1 μM MgATP as compared with GST (Δ_1). However, at a higher concentration of 20 μM MgATP, the exogenous Syn-1A could not further inhibit the K_{ATP} channel current compared with control cells (Δ_2). We summarized these data in Fig. 4, *Bii* and *Cii*. Here, Δ_1 and Δ_2, which indicate reduc-

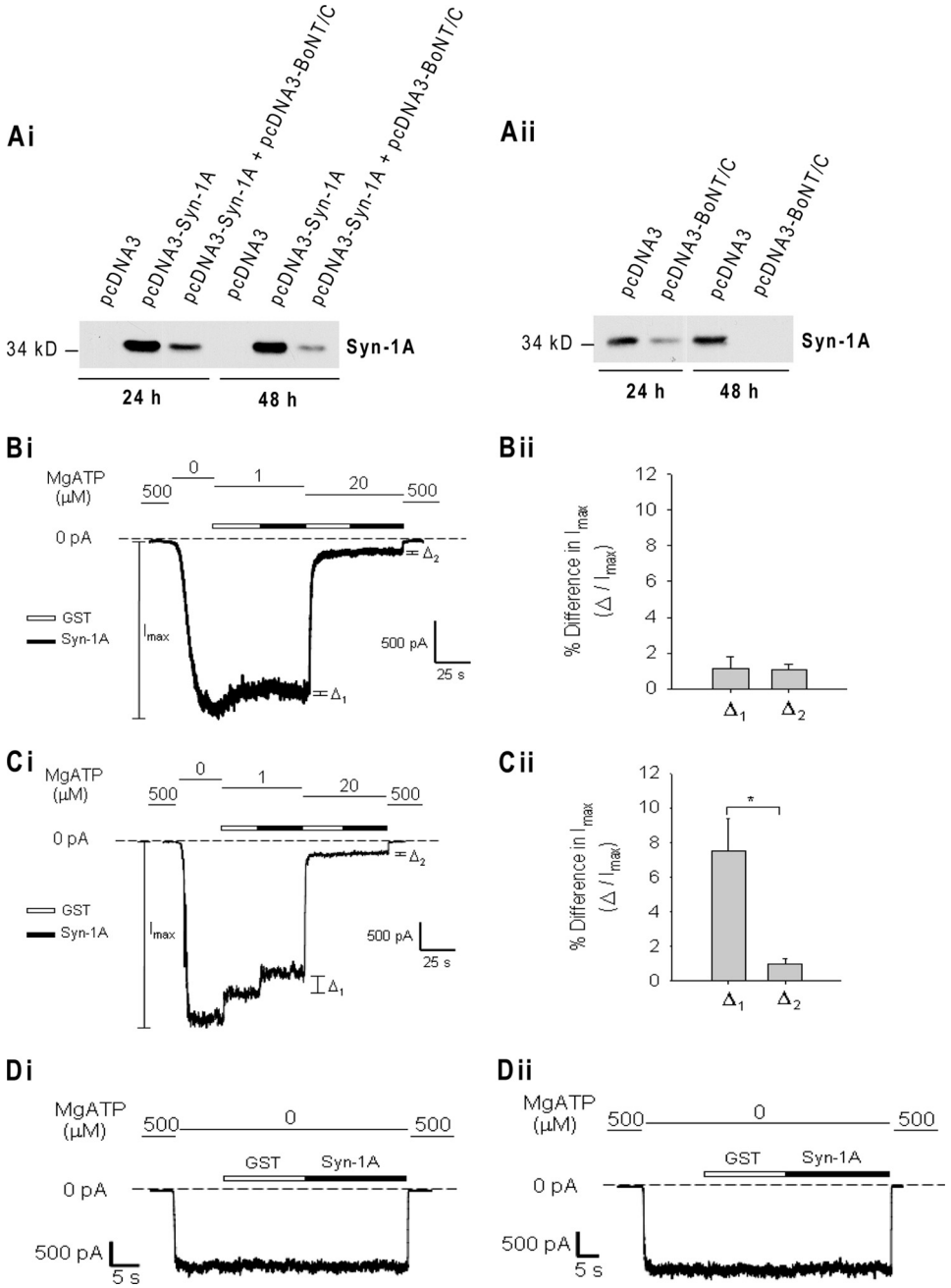

FIGURE 4. **K_{ATP} channel sensitivity to Syn-1A inhibition is enhanced at lower but not at higher ATP concentration in endogenous Syn-1A-depleted cells.** *A*, Western blotting analysis of Syn-1A expression in HEK293 cells transfected with Syn-1A or co-transfected with Syn-1A plus BoNT/C1 (*Ai*), and in INS-1E cells transfected with BoNT/C1 (*Aii*), as indicated. The cells were transfected with empty vector as a control. *B–D*, electrophysiological study. Effects of Syn-1A (0.3 μM) on K_{ATP} channels at various concentrations of ATP were examined. 0.3 μM GST was used as a negative control. *Bi* and *Di*, representative traces obtained from INS-1E cells transfected with EGFP alone. *Ci* and *Dii*, representative traces from INS-1E cells co-transfected with BoNT/C1 and EGFP. *Bii* and *Cii*, summary of results presented as means ± S.E. ($n = 4$). The differences (Δ) in current amplitude between application of GST and Syn-1A were calculated as a percentage of the maximal current (I_{max}) of each individual patch. *, $p < 0.05$.

tion in the K_{ATP} channel current caused by exogenous Syn-1A compared with GST, were calculated as a percentage of the maximal current (I_{max}) of each individual patch. Note that Δ_1 (at 1 μM MgATP) Syn-1A inhibition was much greater in BoNT/C1 transfected cells than the control cells. Our findings therefore show that the effects of ATP on Syn-1A modulation of native K_{ATP} channels is apparent only when endogenous Syn1A is depleted. This suggests that endogenous Syn-1A can rapidly interact with SUR1 when ATP levels are reduced. These results indicate an important role for endogenous Syn-1A and its dynamic interaction with ATP in regulating K_{ATP} channels.

DISCUSSION

Syn-1A is a versatile protein that serves as a platform to which exocytic (30) and ion channel (31, 32) proteins bind and become activated or form functional complexes, consequently modulating the different steps in exocytosis and ion channel gating. Our previous studies have shown that Syn-1A binds to NBF1 and NBF2 domains of SUR subunits to regu-

late K_{ATP} channel activity in both rat pancreatic β-cells (22, 23) and cardiac ventricular myocytes (21, 33). In the present study, we demonstrated that ATP can regulate the physical association of Syn-1A with SUR1 and modulate the inhibitory actions of Syn-1A on K_{ATP} channels. There are two major features. First, ATP is able to dose-dependently inhibit Syn-1A binding to SUR1. Addition of Mg^{2+}, generating MgATP and free Mg^{2+} reduced this ATP-induced inhibition. Second, our electrophysiological studies revealed that ATP modulated K_{ATP} channel sensitivity to endogenous Syn-1A inhibition. Below, we discuss each of these features.

ATP Effects on Syn-1A-SUR1 Physical Interactions—Our results examining the effect of ATP on the physical association between Syn-1A and SUR1 clearly demonstrate an ATP concentration-dependent reduction in the interaction. This ATP-induced inhibitory effect is not dependent on Mg^{2+}, and in fact, addition of Mg^{2+} reduced Syn-1A-SUR1 binding. A number of studies have shown that Mg^{2+} play an important role in regulation of many ion channels, such as the voltage-dependent calcium channel (34) and K_{ATP} channel (9). ATP and ADP regulate K_{ATP} channel activity by interaction with two physically distinct sites on the channel. Interaction with one site causes channel closure, whereas interaction with the other site leads to channel opening (10). The properties of these two sites differ in their requirement for Mg^{2+} (9). Our results show that Mg^{2+} can decrease ATP-induced inhibitory effect on Syn-1A binding to SUR1. Although our finding cannot yet provide the precise Mg^{2+} acting sites on SUR1, we speculate there are three possible explanations for the reduction of ATP-induced Syn-1A binding to SUR1 by Mg^{2+}. The first and most likely explanation is that Mg^{2+} binding to ATP results in reduction of free ATP concentration (see Fig. 1*B*) and the generation of MgATP, the former known to be the potent inhibitor of K_{ATP} channels and the latter to activate the channel (9, 25), thus counteracting the ATP inhibitory effect. Second, Mg^{2+} may alter SUR1 conformation to form a complex with Syn-1A that becomes resistant to ATP inhibition. Third, Mg^{2+} increases the affinity of SUR1 to Syn-1A, but this Syn-1A-SUR1 complex remains receptive to ATP disruption. Further detailed work is needed to investigate how these complex interactions of ATP and Mg^{2+} on SUR1 translate to actual regulation of K_{ATP} channel activity.

When comparing the FRET and binding assays, the ATP sensitivity, in the presence of 2 mM $MgCl_2$ for abolishing the Syn-1A·SUR1 complex, is higher in the FRET study in live cells, particularly at the lower ATP concentration (0.5 mM ATP plus 2 mM $MgCl_2$), wherein disruption of the Syn-1·SUR1 complex was 55.2 *versus* 3.1% for FRET *versus* binding assays, respectively. The reason for this apparent discrepancy may be that Mg^{2+} binds to other endogenous proteins in intact cells employed in the FRET assay; thus, the higher concentration of free ATP would cause a stronger inhibitory effect on Syn-1A binding to SUR1. To address this possibility, we tested whether Mg^{2+} *per se* can affect the Syn-1-SUR1 interaction. As shown in supplemental Fig. 1, 2 mM $MgCl_2$ in itself had no effect on the Syn-1A-SUR1 FRET signal. However, addition of 2 mM $MgCl_2$ to 0.5 mM ATP indeed reduced the ability of 0.5 mM ATP to disrupt the Syn-1A-SUR1 FRET signal. This supports our thinking that Mg^{2+} could affect Syn-1A-SUR1 interaction only in the presence of ATP and that the cytosolic proteins very likely might be chelating endogenous Mg^{2+} as to have caused the increased inhibitory effects of low ATP (0.5 mM ATP) in the FRET experiments. Of course, there may be other undefined reasons.

Physiological Implications—Based on the binding data discussed above, one would predict that at physiological concentrations of ATP, there may be only little Syn-1A binding to SUR1. In inside-out patch recording experiments, Syn-1A modulation of K_{ATP} channel activity was only apparent after depletion of endogenous Syn-1A with BoNT/C1. Taken together, these results suggest that endogenous Syn-1A can rapidly complex with SUR1 in β-cells when ATP levels are lowered. Type 2 diabetes is associated with lower ATP levels in β-cells as a result of diminished efficiency of mitochondrial ATP production in part due to perturbation of uncoupling proteins (35). Here, lower β-cell ATP concentration in diabetes patients would increase K_{ATP} channel sensitivity to Syn-1A-induced inhibition, consequently increasing insulin secretion from pancreatic β-cells during states of low ATP generation, as a compensatory mechanism.

Cytosolic ATP levels undergo considerable changes or lack of changes in health and disease in many cell types (pancreatic islet β- and α-cells, heart, and brain) to regulate their K_{ATP} channels and consequent membrane excitability. The present study demonstrates that Syn-1A and ATP could modulate the sensitivity of K_{ATP} channels to either mediator in an autoregulatory fashion, thus providing a more versatile mechanism to regulate the K_{ATP} channel in different cell types.

REFERENCES

1. Inagaki, N., Tsuura, Y., Namba, N., Masuda, K., Gonoi, T., Horie, M., Seino, Y., Mizuta, M., and Seino, S. (1995) *J. Biol. Chem.* **270,** 5691–5694
2. Suzuki, M., Sasaki, N., Miki, T., Sakamoto, N., Ohmoto-Sekine, Y., Tamagawa, M., Seino, S., Marbán, E., and Nakaya, H. (2002) *J. Clin. Invest.* **109,** 509–516
3. Tarasov, A. I., Girard, C. A., and Ashcroft, F. M. (2006) *Diabetes* **55,** 2446–2454
4. Hou, J. C., Min, L., and Pessin, J. E. (2009) *Vitam. Horm.* **80,** 473–506
5. Clement, J. P., 4th, Kunjilwar, K., Gonzalez, G., Schwanstecher, M., Panten, U., Aguilar-Bryan, L., and Bryan, J. (1997) *Neuron* **18,** 827–838
6. Mikhailov, M. V., Campbell, J. D., de Wet, H., Shimomura, K., Zadek, B., Collins, R. F., Sansom, M. S., Ford, R. C., and Ashcroft, F. M. (2005) *EMBO J.* **24,** 4166–4175
7. Nichols, C. G. (2006) *Nature* **440,** 470–476
8. Locher, K. P. (2009) *Philos. Trans. R. Soc. Lond B. Biol. Sci.* **364,** 239–245
9. Gribble, F. M., Tucker, S. J., Haug, T., and Ashcroft, F. M. (1998) *Proc. Natl. Acad. Sci. U.S.A.* **95,** 7185–7190
10. Hopkins, W. F., Fatherazi, S., Peter-Riesch, B., Corkey, B. E., and Cook, D. L. (1992) *J. Membr. Biol.* **129,** 287–295
11. Proks, P., and Ashcroft, F. M. (2009) *Prog. Biophys. Mol. Biol.* **99,** 7–19
12. Tucker, S. J., Gribble, F. M., Zhao, C., Trapp, S., and Ashcroft, F. M. (1997) *Nature* **387,** 179–183
13. Gribble, F. M., Tucker, S. J., and Ashcroft, F. M. (1997) *EMBO J.* **16,** 1145–1152
14. James, C., Kapoor, R. R., Ismail, D., and Hussain, K. (2009) *J. Med. Genet.* **46,** 289–299
15. Flechtner, I., Vaxillaire, M., Cavé, H., Scharfmann, R., Froguel, P., and Polak, M. (2008) *Best. Pract. Res. Clin. Endocrinol. Metab.* **22,** 17–40
16. Babenko, A. P., Gonzalez, G., and Bryan, J. (1999) *J. Biol. Chem.* **274,**

11587–11592
17. Sharma, N., Crane, A., Clement, J. P., 4th, Gonzalez, G., Babenko, A. P., Bryan, J., and Aguilar-Bryan, L. (1999) *J. Biol. Chem.* **274,** 20628–20632
18. Shyng, S. L., and Nichols, C. G. (1998) *Science* **282,** 1138–1141
19. Webster, N. J., Searle, G. J., Lam, P. P., Huang, Y. C., Riedel, M. J., Harb, G., Gaisano, H. Y., Holt, A., and Light, P. E. (2008) *Endocrinology* **149,** 3679–3687
20. Wu, J., Xu, H., Yang, Z., Wang, Y., Mao, J., and Jiang, C. (2002) *J. Membr. Biol.* **190,** 105–116
21. Kang, Y., Leung, Y. M., Manning-Fox, J. E., Xia, F., Xie, H., Sheu, L., Tsushima, R. G., Light, P. E., and Gaisano, H. Y. (2004) *J. Biol. Chem.* **279,** 47125–47131
22. Pasyk, E. A., Kang, Y., Huang, X., Cui, N., Sheu, L., and Gaisano, H. Y. (2004) *J. Biol. Chem.* **279,** 4234–4240
23. Cui, N., Kang, Y., He, Y., Leung, Y. M., Xie, H., Pasyk, E. A., Gao, X., Sheu, L., Hansen, J. B., Wahl, P., Tsushima, R. G., and Gaisano, H. Y. (2004) *J. Biol. Chem.* **279,** 53259–53265
24. Lin, Y. W., Bushman, J. D., Yan, F. F., Haidar, S., MacMullen, C., Ganguly, A., Stanley, C. A., and Shyng, S. L. (2008) *J. Biol. Chem.* **283,** 9146–9156
25. Ashcroft, F. M., and Kakei, M. (1989) *J. Physiol.* **416,** 349–367
26. Grubbs, R. D. (2002) *Biometals* **15,** 251–259
27. Tramier, M., Zahid, M., Mevel, J. C., Masse, M. J., and Coppey-Moisan, M. (2006) *Microsc. Res. Tech.* **69,** 933–939
28. Ostenson, C. G., Gaisano, H., Sheu, L., Tibell, A., and Bartfai, T. (2006) *Diabetes* **55,** 435–440
29. Lin, C. W., Yan, F., Shimamura, S., Barg, S., and Shyng, S. L. (2005) *Diabetes* **54,** 2852–2858
30. Südhof, T. C., and Rothman, J. E. (2009) *Science* **323,** 474–477
31. Atlas, D. (2001) *J. Neurochem.* **77,** 972–985
32. Leung, Y. M., Kwan, E. P., Ng, B., Kang, Y., and Gaisano, H. Y. (2007) *Endocr. Rev.* **28,** 653–663
33. Kang, Y., Ng, B., Leung, Y. M., He, Y., Xie, H., Lodwick, D., Norman, R. I., Tinker, A., Tsushima, R. G., and Gaisano, H. Y. (2006) *J. Biol. Chem.* **281,** 19019–19028
34. McHugh, D., and Beech, D. J. (1996) *J. Physiol.* **492,** 359–376
35. Zhang, C. Y., Baffy, G., Perret, P., Krauss, S., Peroni, O., Grujic, D., Hagen, T., Vidal-Puig, A. J., Boss, O., Kim, Y. B., Zheng, X. X., Wheeler, M. B., Shulman, G. I., Chan, C. B., and Lowell, B. B. (2001) *Cell* **105,** 745–755